How local flexibility affects knot positioning in ring polymers

Enzo Orlandini,[†,‡] Marco Baiesi,[†,‡] and Francesco Zonta[¶]

†*Department of Physics and Astronomy, University of Padova, Via Marzolo 8, Padova, Italy*

‡*INFN, Sezione di Padova, Via Marzolo 8, Padova, Italy*

¶*Shangai Institute for Advanced Immunochemical Studies (SIAIS), ShanghaiTech University, No. 99 Haike Road, Pudong, Shanghai 201210, China*

E-mail:

Abstract

Recent theoretical findings suggest that the local flexibility of a polymer, linked to the chemical details of the molecule, can affect both the position and the size of knots along the polymer itself. Being of relevance in biology and material science, we further investigate this issue by performing molecular dynamics simulations on a model of diblock flexible-stiff polymer ring hosting a trefoil knot. We show that, when both blocks are sufficiently long to accommodate the knot, by raising the temperature T one may shift the knot position from the flexible part to the stiffer one. Even a very short flexible region has a high probability of lying within the knotted portion at lower temperatures. In addition we observe that there is a tendency for either extremities of the knot to pin at the interface of the two blocks. This correlation between knot position and bending inhomogeneity supports the view that enzymes, binding the DNA in proximity of single-stranded gaps and nicks have a better chance to alter the global topology of the chain. Finally we observe that knots, initially squeezed within flexible portions shorter then the typical knot size, may give rise to long-lived metastable states. [1]

Introduction

Long linear polymers in dilute solution can be self-entangled and knots can be found in circular chains ensuing from a ring closure.[1] This phenomenon is relevant in molecular biology: topological entanglement would prevent the segregation of DNA after replication in bacteria, and specific enzymes such as topoisomerases and recombinases [2–4] are needed to eliminate knots and linking between the two DNA strands. The presence of knots also influences the the spatial organization of viral DNA condensed in capsids.[5,6]

In the last years, properties such as the knotting probability, the knot complexity and the knot average size of models of circular polymers have been extensively studied as a function of the chain contour length, the solvent quality as well as the degree of spatial confinement and the strength of mechanical constraints.[1,7–15]

Despite the advances in determining the degree of complexity and localization of the knot in the whole polymer, the interplay between these global topological properties and the chemical details of the polymer itself is not completely understood. The degree of flexibility of the polymer, for example, is known to affect its

[1]This document is the unedited Author's version of a Submitted Work that was subsequently accepted for publication in Macromolecules, copyright

knotting probability,[15–17] but only recently it has been put in some relationship with a spatial confinement of the knotted part.[14,18] Indeed, it has been demonstrated that for a knotted linear chain under stretching there exists an optimal stiffness at which the free-energy of the knotted state, relative to that of the unknotted state, is minimal. This would suggest that for equilibrated knotted polymer chains, made by regions of different stiffness, the knot would reside with high probability in the region with the stiffness closer to the optimal one, at least if such region is long enough to host the knot.[18] Stiffness heterogeneity occurs for example in diblock copolymers made by a rigid rod and a flexible tail that self-assemble into novel macroscopic soft structures. These systems have many potential applications in organic electronics and biotechnology.[19,20] Stiffness heterogeneity is a frequent feature also in DNA molecules: for example, in double-stranded DNA (ds-DNA) a region of the backbone rich of AT base pairs is roughly twice more flexible than a corresponding CG-rich region.[21] Moreover, the persistence length $l_p \approx 50$nm of the double helix of DNA is roughly five times larger than that of single stranded DNA. The latter is found for instance in local opening of base pairs due to thermal fluctuations[22,23] These local softenings may have important implications in the process of topological simplification of knotted circular ds-DNA. Indeed there is recent evidence that topoisomerases prefer to bind to softer regions of DNA,[24] whose knots tend to localize in the vicinity of single-stranded gaps.[25]

These observations motivate us to address the question of how a local property of the polymer, its (heterogeneous) stiffness, can affect topological properties such as the position and size of knots within a circular knotted polymer. For simplicity, we will restrict ourselves to stiff-flexible diblock rings where the circular polymer chain of total contour length L is composed by two portions, one fully flexible and the other stiff (technically, "semiflexible") with a given persistence length l_p. For this system, two length scales can be naturally identified: the persistence length l_p and the contour length of the stiff sub-chain L_s or, complementary, the contour length of the flexible block $L_f = L - L_s$. For knotted diblock rings an additional length scale, associated to the average size of the knotted region, must be considered and, by the interplay of these length scales, many different scenarios may occur.

Here we focus on three typical cases, all relative to stiff-flexible diblock copolymer rings hosting a 3_1 knot (the simplest knot[1]): (i) rings where the two halves are equally long ($L_f = L_s$) and sufficiently large to accommodate the knot in its relaxed state, (ii) rings where the flexible block is too short to accommodate the knot even in its minimal size conformation, and (iii) diblock rings where the flexible part has a contour length that is just below the natural knot size. These different setups complement each other and give an overview of the possible scenarios for knot positioning in ring polymers with heterogeneous stiffness. The paper is organized as follows: the model and the simulation settings are described in section *Model and methods*. In section *Results* all our findings are presented according to the above mentioned cases. Finally, the *Conclusions* section is devoted to a summary of the main results and to conclusions.

Model and methods

The circular polymer is modeled as a ring of N beads of mass $m = 1$ and diameter σ. With this coarse-grained description the polymer contour length is given by $L = N\sigma$. In the following, the position in space of the center of the ith bead is indicated by $\vec{r}_i$ while the distance vector of beads i and j is denoted as $\vec{d}_{i,j} = \vec{r}_i - \vec{r}_j$ and its norm as $d_{i,j}$. The steric interaction (self-avoidance) between beads is taken into account by a truncated and shifted Lennard-Jones potential (also known as Weeks-Chandler-Anderson potential)

$$U_{\mathrm{LJ}} = 4\epsilon \left[\left(\frac{\sigma}{d_{i,j}} \right)^{12} - \left(\frac{\sigma}{d_{i,j}} \right)^{6} + \frac{1}{4} \right] \theta(2^{1/6}\sigma - d_{i,j}) \, . \tag{1}$$

where $\theta(x)$ is the Heaviside function and ϵ is the characteristic unit of energy of the system that is set equal to the thermal energy k_BT. The connectivity of the chain is enforced by the finitely extensible non-linear elastic (FENE[26]) potential acting between two consecutive beads $(i, i+1)$

$$U_{\rm FENE}(i,i+1) = -\frac{\alpha}{2}R_0^2 \ln\left[1-\left(\frac{d_{i,i+1}}{R_0}\right)^2\right], \quad (2)$$

for $d_{i,i+1} < R_0$ and $U_{\rm FENE}(i,i+1) = \infty$ otherwise; here we choose $R_0 = 1.5\sigma$ (so that crossing of bonds does not occur in the simulations) and $\alpha = 30\epsilon$. In our simulation the temperature is given in units of ϵ/k_B with $\epsilon = k_B = 1$.

Each ring is partitioned into two blocks, one flexible with N_f beads and one stiff with $N_s = N - N_f$ beads. The bending rigidity of the stiff block is expressed by the bending energy potential

$$U_{\rm bend} = \sum_{i=2}^{N_s} \kappa \left(1 - \frac{\vec{b}_{i-1}\cdot\vec{b}_i}{|\vec{b}_{i-1}|\,|\vec{b}_i|}\right), \quad (3)$$

where $\vec{b}_i \equiv \vec{r}_{i+1} - \vec{r}_i$ is the i-th chain bond and the stiffness constant is fixed to $\kappa = 20\epsilon = 20$ (the flexible block does not contribute to the bending energy). Hence, to change the persistence length of the stiff block we use the procedure of varying the temperature, exploiting the relation $l_p = \kappa\sigma/T$. Note that by choosing $\sigma = 2.5$nm (the diameter of a hydrated ds-DNA strand) the case $T = 1$ would correspond to ds-DNAs with $l_p = 50$nm, the expected value of this molecule for solutions with high ionic strength.

The kinetics of the rings is studied using fixed-volume and constant temperature molecular dynamics simulations with implicit solvent. The dynamics was integrated numerically using the LAMMPS package[27] with a Langevin thermostat. Periodic boundary conditions are applied with the simulation box large enough to avoid chain self interactions across the boundaries. The elementary integration time is $\Delta t = 0.001\tau_{\rm LJ}$ with $\tau_{\rm LJ} = \sigma\sqrt{m/\epsilon}$ and the friction coefficient γ corresponds to $\gamma/m = 0.5/\tau_{\rm LJ}$.

To test the ergodicity of the system with respect to the position of the knot within the diblock ring, we often consider two different initial configurations: (i) the 3_1 knot is generated on the surface of a wide torus such that it is spread along the whole ring; (ii) the knot is localized within a short portion (≈ 24 monomers) of the N_f flexible block. When not explicitly specified, it is understood that the long time dynamics is independent of the two initial conditions and the results obtained from both simulations are combined together.

For a given initial condition and temperature, T, we perform a long molecular dynamics trajectory and we monitor the time evolution of the position and size of the knotted region. The identification of the knotted region within the ring is in general a non trivial task to perform due to the intrinsic difficulty of providing a consistent definition of the knotted arc within a curve.[1] This produces some sensitivity of the determination of the knot position to the particular search scheme.[28] Here we rely on a detection algorithm that was introduced by Marcone et al.[29] (refined by Tubiana et al.[28]) to measure the equilibrium size of knots in polymer rings in good solvent solution, which later proved to work very efficiently in different situations.[30,31] In this method, for a given knotted ring, various open portions are considered and, for each of these, a closure is made by joining its ends with a path designed to minimally interfere with the portion itself. The knotted arc is then identified with the shortest portion still displaying the original knot type (i.e., sharing the same Alexander polynomial[32]).

For sufficiently long trajectories, one can also compute statistical properties of the knot location in terms, for example, of the probability distribution function of the position of the knot extremities along the ring. The whole procedure took some months of CPU time for each studied case. We obtained $2.5 \div 5 \times 10^3$ samples for each temperature. If autocorrelation times relative to the knot size are considered, in the worst case these data reduce to a few hundreds of uncorrelated configurations. By comparing the outcome of two independent runs, we see that a good degree of ergodicity in the sam-

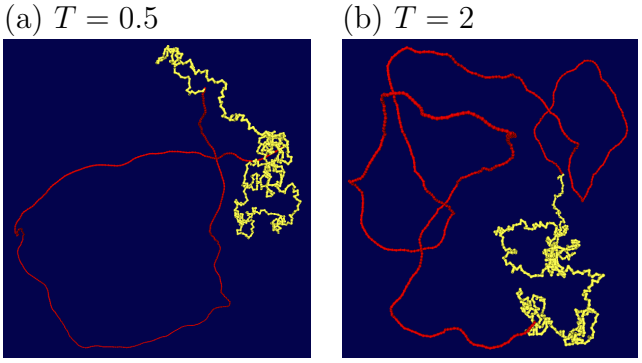

Figure 1: Snapshots at (a) $T = 0.5$ and (b) $T = 2$ of rings with $N = 1000$ monomers, divided in a stiff half (red) and a flexible half (yellow). The configuration at $T = 0.5$ does not display the knot in the stiff half (hence it must be in the yellow random coil), while the knot is visible in the stiff half of the configuration (b), on the left. Note also the lower persistence length of the stiff part in the snapshot at higher T.

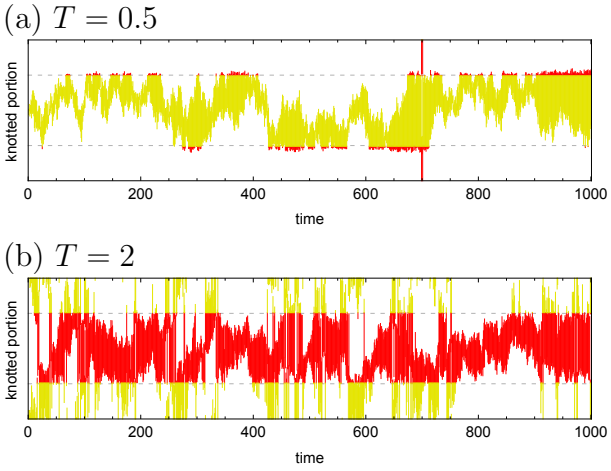

Figure 2: Typical trajectory of the knotted region within a circular chain of total length $N = 1000$ and flexible/stiff halves of equal length ($N_s = N_f = 500$), for (a) $T = 0.5$ and (b) $T = 2$ cases. Red and yellow colors highlight the bead indices belonging respectively to the stiff and flexible halves of the ring.

pling is usually achieved. In subsection *Knot trapping and multistability* will deal with an interesting counterexample, in which metastable states are found.

Results

Flexible-Rigid diblock knotted rings

We first discuss whether and to which extent a temperature-induced change in the bending rigidity of the stiff sub-chain affects the equilibrium size and location of the knotted region of the ring polymer. Let us start by looking at rings with $N = 1000$ monomers partitioned into a stiff and flexible region of equal size ($N_s = N_f = 500$). Since the typical contour length of a knotted region hosted in a flexible chain of length $N = 1000$ is expected to be less than 500,[33] in this case the knotted region should be comfortably hosted in either halves of the ring. Indeed the mean knot sizes are reasonably below $N/2$: their estimates taken at various temperatures are ≈ 300 ($T = 0.5$), ≈ 380 ($T = 1$ and 1.5), and ≈ 340 ($T = 2$). The two snapshots shown in Figure 1 show typical configurations, one at $T = 0.5$ (Figure 1(a)) and one at $T = 2$ (Figure 1(b)).

In Figure 2 we report a typical steady state trajectory of the knot along the ring for two different values of the temperature [$T = 0.5$, Figure 2(a) and $T = 2$, Figure 2(b)], namely, two different rigidities of the stiff block. The colored region refers to the set of beads belonging to the knotted region: the yellow and red code refer to beads respectively of the flexible and stiff portion of the ring. As the indexing of the beads is arbitrary and periodic (the chain is circular), in the figures we shift indices for best visualizing the knotted region. One can notice that for both temperatures the knot size fluctuates in an appreciable way but it rarely reaches lengths $\approx N/2$. At low temperature, where the stiff block is more rigid, the knotted region always resides within the flexible region. Such clear cut dynamical pattern is not present at $T = 2.0$, although the propensity of the knot to reside in the stiff region seems higher.

To better quantify the knot tendency to situate in a given block at a given temperature T, we estimate the probability density $\rho(i, T)$ that the i-th bead of the ring belongs to the knotted region. In Figure 3(a) we show $\rho(i, T)$ for different values of T (i.e., effectively, dif-

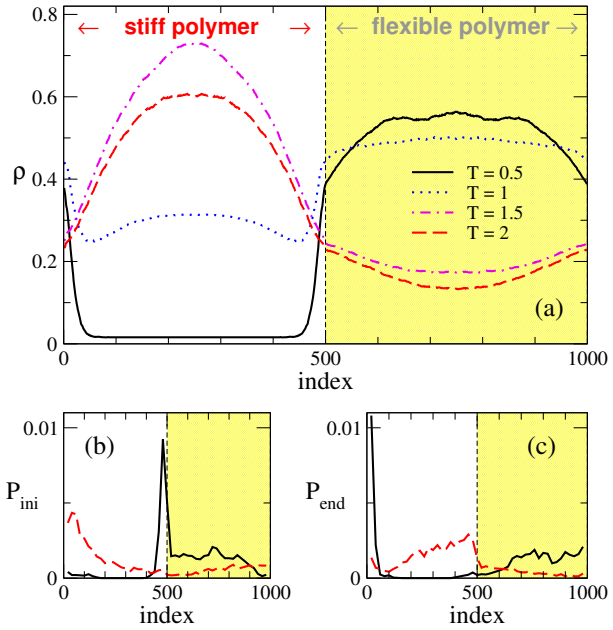

Figure 3: (a) Profile of the frequency of knot per monomer, at four temperatures (see legend), for a loop copolymer of length $N = 1000$ with $N_s = 500$ stiff monomers (white region) and $N_f = 500$ flexible monomers (yellow region). Note that the knot prefers to sit in either the flexible portion at low T or in the stiff part at high T. The profile at $T = 2$ is everywhere lower than that at $T = 1.5$ because the knot is on average shorter at the higher temperature. In the two panels below we plot the probability of finding the first (b) or the last (c) monomer of the knot in given position i of the diblock ring.

ferent values of the bending stiffness in the stiff part). As one could easily anticipate by looking at Figure 2(a), the distribution $\rho(i, T)$ is biased towards the flexible region when the stiff subchain has a long persistence length. This confirms that the most probable equilibrium low-T configurations are those in which the knot is within the flexible sub-chain. The situation is reversed by raising the temperature: at $T \simeq 1.5$ the density $\rho(i, T)$ becomes more peaked in the stiff region, signaling a preference of the knotted region to sit on the stiffer half of the ring.

We can explain this temperature-driven flipping of the knot location by considering recent results for a model of stiff linear knotted chain under tension: Matthews et al.[18] found that the free energy cost of forming a knot attains a minimum for a finite value of the bending rigidity. This value depends on the tension applied at the chain extremities. By extrapolating to the zero tension limit the values shown in Figure 4 of Ref.[18] for $N = 512$, one obtains a value of $\kappa_{min}/k_BT \approx 10$ that is compatible with the value we obtain for $T \approx 1.5$, i.e., $\kappa_{min} = 20/T_{min} = 20/1.5 \approx 13$.

The time series in Figure 2(a) suggests another peculiar feature: for stiff portions that are sufficiently rigid ($T = 0.5$ for example) the knotted region not only resides most of the time in the flexible region, with the flexible-stiff junctions acting as reflecting boundaries, but its position is more biased towards the proximity of one of the two junctions. In fact one of the knot extremities is often pinned on the stiff side of the border (see the small red spots at the border of the yellow regions in Figure 2(a)). This effect can be quantified by estimating the probability of finding the first or last monomer of the knot in a given position i along the ring. These are plotted Figure 3(b) and Figure 3(c), respectively. The peaks in these distributions confirm that one extremity of the knotted region is most likely located just outside the flexible region.

Knotted rigid rings with a soft defect

In the statistics considered so far both halves were equally long and each large enough to accommodate the fluctuating knot. The opposite situation occurs when, for example, the flexible region is too short to fully accommodate the knot. This can arise in knotted ds-DNA when small denatured bubbles are formed by thermal fluctuation well below the denaturation temperature. We check the extent to which the presence of a softer small region (i.e., a kind of soft defect) in an otherwise stiff ring can influence the statistics of the knot size and position. In this respect we consider a trefoil diblock copolymer ring with $N_s = 490$ beads forming the stiff block and only $N_f = 10$ for the flexible one. Snapshots for this configuration at $T = 0.5$ are shown in Figure 4. Since almost the whole ring is quite rigid at low T, in this case we could not achieve a good and

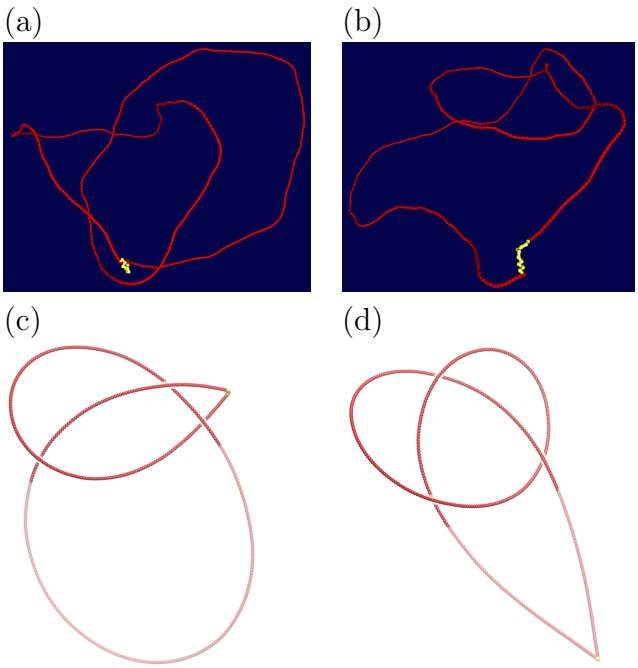

Figure 4: Snapshots of rings with $N = 500$ monomers at $T = 0.5$. In (a) the knot encloses the short flexible (yellow) segment, while in (b) such segment is outside the knotted region. (c) Smooth version of (a) representing the ensemble of configuration in C1 (see the text). (d) Smooth version of (b), representing the ensemble of configuraton in C2. In (c)-(d) the darker part includes the knot.

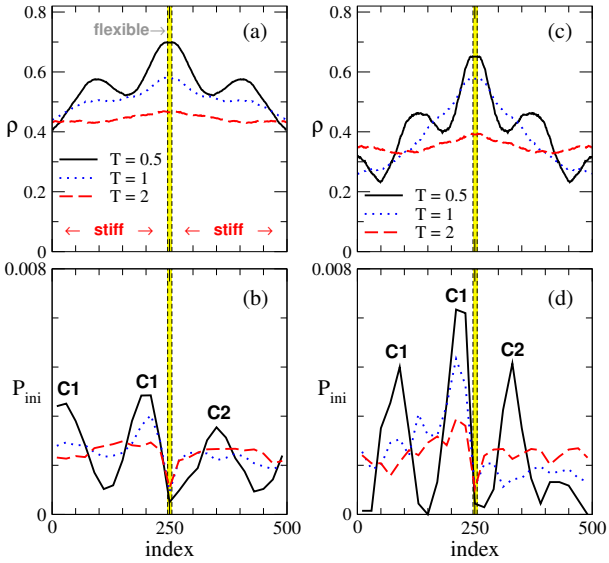

Figure 5: (a) Profile of the frequency of knot per monomer for a loop copolymer of length $N = 500$ with $N_f = 10$ flexible monomers (yellow strip). (b) Probability of finding the first monomer of the knot in a monomer. Being the knot on average ≈ 280 monomers long, at both peaks marked with C1 at $T = 0.5$ the flexible portion is within the knot and near its end [e.g., as in Figure 4(a)], while in configuration C2 the flexible part is not included in the knot [Figure 4(b)]. (c)-(d) As in (a)-(b) but statistics based only on configurations with knots of length at most 225, that is 45% of the chain length.

robust sampling of equilibrated configurations just by running basic Langevin molecular dynamics. We have thus coupled the molecular dynamics simulation with the multiple-Markov chain (or replica) technique, in which several temperatures are simulated in parallel and one allows swapping between configurations at different temperatures.[34] This procedure has the well known advantage of increasing the mobility of the stochastic sampling also at very low T and to furnish the equilibrium statistics within a wide range of temperatures at once.

In Figure 5(a) we show the behaviour of the knot density $\rho(i, T)$ at a few sampled temperatures. It appears clear that the flexible region has, on average, a remarkably high probability to be within the knot. This is confirmed by comparing the fraction of configurations having the knotted part including the flexible region with the same fraction for knotted portions of the same length randomly placed along the ring, see Figure 6. As the temperature is lowered the fraction becomes significantly higher than the randomized counterpart. Moreover the probability of finding the first monomer of the knot at a given position is strongly modulated by the presence of the defect, see Figure 5(b). There, the two peaks C1 represent configurations where the knot most likely include the flexible defect (e.g., such as in Figure 4(a) and (c)). On the other hand, configurations with a knot starting at the C2 peak exclude the defect from the knot (e.g., Figure 4(b) and (d)). While C2 is symmetric with respect to the flexible part (Figure 4(d)), note that C1 in Figure 4(c) can be realized by configurations in which the knotted region either starts just after or ends immediately before the flexible

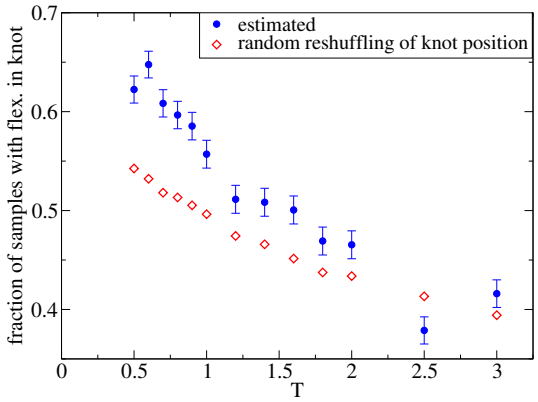

Figure 6: Probability of finding the $N_f = 10$ flexible monomers within the knot, compared to that of knots of equal length placed randomly along the chain ($N = 500$), as a function of temperature.

part (an orientation of the polymer backbone is understood). Thus, the two C1 peaks in Figure 5(a) represent the same kind of configurations, although they have different heights due to statistical fluctuations.

This pattern is enhanced if one consider only knots of length up to 45% of the chain length (225 monomers), see Figure 5(c) and Figure 5(d). Since the pattern C1 is more represented than C2, we observe that a copolymer endowed with a soft defect relaxes tension (with respect to a totally stiff chain) preferentially by including the soft part within the knot.

Knot trapping and multistability

Above we have shown that the knotted region at low temperatures equilibrates within the softer portion of the ring, if this portion is long enough. Further interesting features arise whenever this portion is not sufficiently long to easily accommodate the knot in its unconstrained form. The squeezing of a delocalized knot in the softer region is a process that should require overcoming a free-energy barrier. At low temperatures this barrier may be very high. Hence, due to the competition between the bending rigidity and the configurational entropy of the knot at low T, one expects the formation metastable states that crucially depend on the initial conditions.

In order to explore this issue we consider a

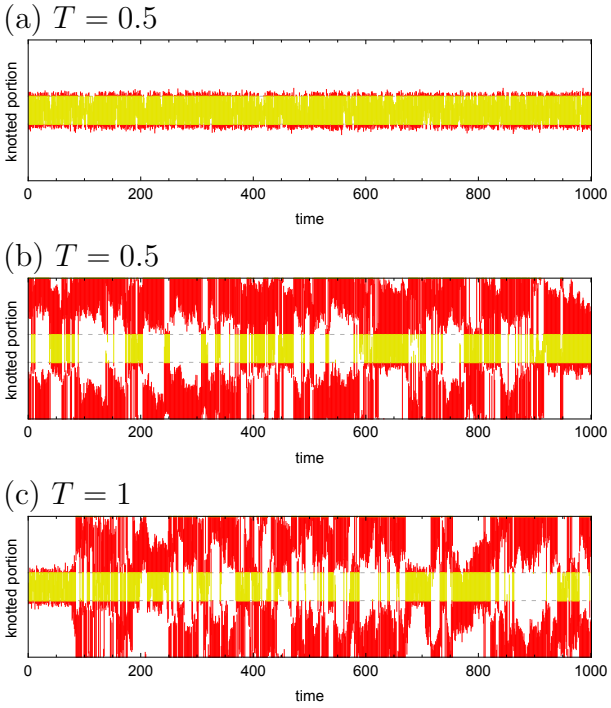

Figure 7: Time series of the knotted region for $N = 500$ and $N_f = 100$. (a) Simulation at (low) $T = 0.5$, started from a knot localized within the N_f monomers of the flexible polymer (yellow region) and (b) from a fully delocalized knot. (c) Simulation similar to (a) but at a higher temperature, $T = 1$: in this case the thermal energy allows the knot to escape from the flexible part, and to eventually return there freely (e.g., at time ≈ 700).

$N = 500$ diblock trefoil ring with a $N_f = 100$ flexible region, well below the expected knot natural size $N_k \approx 180$ (this estimate has been obtained by simulating a fully flexible trefoil ring of $N = 500$ and measuring the average size of the knotted region). For this system we follow the dynamical trajectories at the fixed temperature $T = 0.5$ by considering two particular conditions: one in which the trefoil is initially tied within the flexible block, and the other where the knot is spread across the whole ring (fully delocalized). Figure 7 shows the trajectory of the knotted region when the knot is initially localized in the flexible block, see panel (a), or fully delocalized, panel (b). One can readily see that the localized knot remains trapped within the softer region while the delocalized one resides most

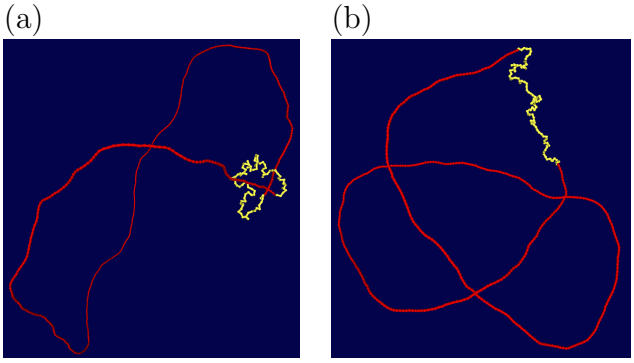

Figure 8: Snapshots of rings with $N = 500$ monomers, of which $N_f = 100$ form the flexible part (yellow) and $N_s = 400$ form the stiff part (red), at low $T = 0.5$. (a) Snapshot from a simulation started with the knot fully within the flexible part; the stiff part acts as a bow with strength increasing with $1/T$. (b) From a simulation started with a delocalized knot.

of the time in the rigid counterpart, leaving the flexible block unaffected. Typical configurations of these two long-lived states are given in Figure 8(a) and (b). These results emerge because the rigidity of the stiff block is relevant at this temperature: the stiffer segments could not be passed through the flexible knot, or bent sufficiently to transmit the knot from the stiff portion to the flexible one, and vice versa . At higher temperatures such phenomenon disappears, as shown for $T = 1$ in Figure 7(c). In this case the relative rigidity between the flexible and stiff regions is low enough, the tension at the boundaries weakens, and we observe a relaxation of the knot towards its natural size and its free trespassing in the stiff part.

Conclusions

We have shown that the interplay between stiffness heterogeneity and topology in flexible-stiff diblock knotted rings gives rise to non trivial scenarios in the size and location of the topological entanglement. In particular the dynamics and the equilibrium statistics of the knotted region within the ring depends on several factors, such as the rigidity of the stiff block and the length of the flexible one compared to the natural length of the knotted region.

For sufficiently long stiff and flexible blocks the equilibrium statistics of the knot position depends on the persistence length of the stiff block, as expected from free energy arguments.[14,18] At low temperatures, where the stiff polymer has a large persistence length, the knot prefers to sit in the flexible part. The situation is reversed by raising the temperature. Hence, in principle, a topological relocation along the copolymer may be achieved by changing the solvent temperature or any parameter affecting the persistence length of the stiff block.

When the length of the flexible block is too small to accommodate the knot, we still detect a marked increase in the probability of finding it within the knotted region, often near one of its two boundaries.

In general we note that the boundaries between the two blocks of different rigidities are frequently overlapped with the extremities of the knotted region. This correlation between knot position and sharp bending variation in the ring could enable a local mechanism of knot identification by topoisomerases in addition to the ones already suggested in literature.[35,36] Essentially, topoisomerases finding bending variations should have an enhanced probability to meet also knotted regions. Another interesting picture emerges when the length of the flexible block is not negligible yet smaller than the natural knot size. We detect the presence of metastable states that differ by the location and size of the knot and whose lifetimes depend on the relative length and rigidity of the two blocks. At sufficiently low temperature, a very intriguing trapping of a squeezed knot is observed within the flexible block, if the knot is initially located there: Within the timescale of our simulations, the squeezed knot forms a metastable state and a breaking of ergodicity occurs. This multistability can offer a good method to control the size and position of the topological entanglement.

Hence, there emerges the possibility of using the parameter temperature for switching from one (metastable) state to another, and to condition the location and size of the knot along the ring. This is worth further investigation.

References

(1) Orlandini, E.; Whittington, S. G. Statistical topology of closed curves: Some applications in polymer physics. *Rev. Mod. Phys.* **2007**, *79*, 611–642.

(2) Wassermann, S. A.; Cozzarelli, N. R. Biochemical topology: applications to DNA recombination and replication. *Science* **1986**, *232*, 951–960.

(3) Rybenkov, V.; Ullsperger, C.; Vologodskii, A. V.; Cozzarelli, N. R. Simplification of DNA topology below equilibrium values by type II topoisomerases. *Science* **1997**, *277*, 690–693.

(4) López, V.; Martínez-Robles, M.-L.; Hernández, P.; Krimer, D. B.; Schvartzman, J. B. Topo IV is the topoisomerase that knots and unknots sister duplexes during DNA replication. *Nucleic Acids Research,* **2011**, *40*, 3563–3573.

(5) Arsuaga, J.; Vázquez, M.; Trigueros, S.; Sumners, D. W.; Roca, J. Knotting probability of DNA molecules confined in restricted volumes: DNA knotting in phage capsids. *Proc. Natl. Acad. Sci. USA* **2002**, *99*, 5373–5377.

(6) Marenduzzo, D.; Orlandini, E.; Stasiak, A.; Sumners, d. W.; Tubiana, L.; Micheletti, C. DNA-DNA interactions in bacteriophage capsids are responsible for the observed DNA knotting. *Proc Natl Acad Sci U S A* **2009**, *106*, 22269–22274.

(7) Micheletti, C.; Marenduzzo, D.; Orlandini, E. Polymers with spatial or topological constraints: Theoretical and computational results. *Physics Reports* **2011**, *504*, 1.

(8) Virnau, P.; Kantor, Y.; Kardar, M. Knots in globule and coil phases of a model polyethylene. *J. Am. Chem. Soc.* **2005**, *127*, 15102–15106.

(9) Matthews, R.; Louis, A. A.; Yeomans, J. M. Effect of topology on dynamics of knots in polymers under tension. *Europhys. Letts.* **2010**, *89*, 20001.

(10) Baiesi, M.; Orlandini, E.; Whittington, S. G. Interplay between writhe and knotting for swollen and compact polymers. *J. Chem. Phys.* **2009**, *131*, 154902.

(11) Baiesi, M.; Orlandini, E.; Stella, A. L.; Zonta, F. Topological signature of globular polymers. *Phys. Rev. Lett.* **2011**, *106*, 258301.

(12) Micheletti, C.; Orlandini, E. Knotting and metric scaling properties of DNA confined in nano-channels: a Monte Carlo study. *Soft Matter* **2012**, *8*, 10959–10968.

(13) Dai, L.; van der Maarel, J. R. C.; Doyle, P. S. Effect of Nanoslit Confinement on the Knotting Probability of Circular DNA. *ACS Macro Letters* **2012**, *1*, 732–736.

(14) Poier, P.; Likos, C. N.; Matthews, R. Influence of Rigidity and Knot Complexity on the Knotting of Confined Polymers. *Macromolecules* **2014**, *47*, 3394–3400.

(15) Virnau, P.; Rieger, F. C.; Reith, D. Influence of chain stiffness on knottedness in single polymers. *Biochem. Soc. Trans.* **2013**, *41*, 528–532.

(16) Orlandini, E.; Tesi, M. C. Knotted polygons with curvature in Z(3). *J. Phys. A: Math. Gen.* **1998**, *31*, 9441–9454.

(17) Orlandini, E.; Tesi, M. C.; Whittington, S. G. Entanglement complexity of semiflexible lattice polygons. *J. Phys. A: Math. Gen.* **2005**, *38*, L15–L21.

(18) Matthews, R.; Louis, A. A.; Likos, C. N. Effect of Bending Rigidity on the Knotting of a Polymer under Tension. *ACS Macro Letters* **2012**, *1*, 1352–1356.

(19) Chen, J. T.; Thomas, E. L.; Ober, C. K.; Mao, G. Self-Assembled Smectic Phases

in Rod-Coil Block Copolymers. *Science* **1996**, *273*, 343–346.

(20) Segalman, R. A.; McCulloch, B.; Kirmayer, S.; Urban, J. J. Block Copolymers for Organic Optoelectronics. *Macromolecules* **2009**, *42*, 9205–9216.

(21) Hogan, M.; Legrange, J.; Austin, B. Dependence of DNA helix flexibility on base composition. *Nature* **1983**, *304*, 752–754.

(22) Ramstein, J.; Lavery, R. Energetic coupling between DNA bending and base pair opening. *Proc. Natl. Acad. Sci. USA* **1988**, *85*, 7231–7235.

(23) Chen, H.; Meisburger, S. P.; Pabit, S. A.; Sutton, J. L.; Webb, W. W.; Pollack, L. Ionic strength-dependent persistence lengths of single-stranded RNA and DNA. *Proc. Natl. Acad. Sci. USA* **2012**, *109*, 709–804.

(24) Dong, K. G.; Berger, J. M. Structural basis for gate-DNA recognition and bending by type IIA topoisomerases. *Nature* **2007**, *450*, 1201–1205.

(25) Racko, D.; Benedetti, F.; Dorier, J.; Burnier, Y.; Stasiak, A. Generation of supercoils in nicked and gapped DNA drives DNA unknotting and postreplicative decatenation. *Nucleic Acids Res.* **2015**,

(26) K. Kremer, G. G. Dynamics of entangled linear polymer melts: A molecular dynamics simulation. *J. Chem. Phys.* **1990**, *92*, 5057–5086.

(27) Plimpton, S. LAMMPS. *J. Comput. Phys.* **1995**, *117*, 1.

(28) Tubiana, L.; Orlandini, E.; Micheletti, C. Profiling the arc entanglement of compact ring polymers: a comparison of different arc-closure schemes with applications to knot localization. *Prog. Theor. Phys.* **2011**, *191*, 192–204.

(29) Marcone, B.; Orlandini, E.; Stella, A. L.; Zonta, F. What is the length of a knot in a polymer? *J. Phys. A: Math. Gen.* **2005**, *38*, L15–L21.

(30) Marcone, B.; Orlandini, E.; Stella, A. L.; Zonta, F. Size of knots in ring polymers. *Phys. Rev. E* **2007**, *75*, 041105–11.

(31) Tubiana, L.; Orlandini, E.; Micheletti, C. Multiscale Entanglement in Ring Polymers under Spherical Confinement. *Phys. Rev. Lett.* **2011**, *107*, 188302.

(32) Adams, C. C. *The Knot Book*; Freeman, 1994.

(33) Tubiana, L.; Rosa, A.; Fragiacomo, F.; Micheletti, C. Spontaneous Knotting and Unknotting of Flexible Linear Polymers: Equilibrium and Kinetic Aspects. *Macromolecules* **2013**, *46*, 3669–3678.

(34) Tesi, M. C.; Janse Van Rensburg, E. J.; Orlandini, E.; Whittington, S. G. Monte Carlo study of the interacting self-avoiding walk model in three dimensions. *J. Stat. Phys.* **1996**, *82*, 155–181.

(35) Liu, Z.; Zechiedrich, E. L.; Chan, H. S. Inferring Global Topology from Local Juxtaposition Geometry: Interlinking Polymer Rings and Ramifications for Topoisomerase Action. *Biophysical J.* **2006**, *90*, 2344–2355.

(36) Liu, Z.; Deibler, R. W.; Chan, H. S.; Zechiedrich, E. L. The why and how of DNA unlinking. *Nucleic Acids Research* **2009**, *37*, 661–671.